A Front-Fixing ETD Numerical Method for Solving Jump-Diffusion American Option Pricing Problems

Rafael Company[a,*], Vera N. Egorova[b], Lucas Jodár[a]

[a] *Instituto de Matemática Multidisciplinar, Universitat Politècnica de València, Camino de Vera, s/n, 46022 Valencia – Spain*
[b] *Departamento de Matemática Aplicada y Ciencias de la Computación, Universidad de Cantabria, Avda. de los Castros, s/n, 39005 Santander – Spain*

Abstract

American options prices under jump-diffusion models are determined by a free boundary partial integro-differential equation (PIDE) problem. In this paper, we propose a front-fixing exponential time differencing (FF-ETD) method composed of several steps. First, the free boundary is included into equation by applying the front-fixing transformation. Second, the resulting nonlinear PIDE is semi-discretized, that leads to a system of ordinary differential equations (ODEs). Third, a numerical solution of the system is constructed by using exponential time differencing (ETD) method and matrix quadrature rules. Finally, numerical analysis is provided to establish empirical stability conditions on step sizes. Numerical results show the efficiency and competitiveness of the FF-ETD method.

Keywords: American option pricing, front-fixing method, exponential time differencing, finite difference methods, experimental numerical analysis, Gauss quadrature
2010 MSC: 60G40, 65N06, 65N12

1. Introduction

It is generally accepted today that jump-diffusion models are one of the appropriate ways to capture the empirical market data not reproduced by the

*Corresponding author: vera.egorova@unican.es

Black-Scholes model of option pricing [1, 2].

In jump-diffusion models, in both cases of finite or infinite activity, the option price function can be expressed as the solution of a partial integro-differential problems (PIDEs) [3]. Among the most important models of finite activity we mention the Merton model whose jump amplitudes are represented by log-normally distributed processes [4], and the Kou model where the jump amplitudes follow log-double-exponential distributed processes [5].

For the sake of interest in the applications of jump-diffusion models, it is more interesting the more complex American option case. Such model has two main approaches, the linear complementarity problem (LCP) formulation and the front-fixing method [6]. Probably the most used approaches are the LCP with the penalty term [7, 8, 9], and the operator splitting method [10, 11].

Dealing with jump-diffusion models, the front-fixing method has the advantage that allows the computation of the optimal exercise boundary and the challenge of consider a nonlinear PIDE with an additional variable [12, 13].

Broadie and Kaya [14], and D'Ippoliti et al. [15] use Monte-Carlo techniques to deal with jump-diffusion models with stochastic volatility. A finite-element method combined with a front-fixing approach is proposed in [13]. Ballestra and Sgarra use a finite element method with an operator splitting approach in [16]. A pseudo-spectral method is proposed in [17].

Finite-difference (FD) methods and the method of lines are proposed by Chiarella et al. in [18]. FD schemes using implicit iterative methods are proposed in [19]. Implicit-explicit (IMEX) finite difference methods are suggested in [20].

Mesh-less methods of radial basis functions (RBF) type have been employed in [12] after applying the front-fixing technique and in [21] combining the RBF with IMEX operator splitting method. FD scheme for RBF method is proposed in [22] for Merton and Kou's models. Penalty approach together with RBF method is used in [9], where for the full discretization a fitted finite volume method is employed.

In the present paper, we consider two of the most used jump-diffusion models: Merton model based on lognormal distribution [4], and Kou's model represented by a log-double-exponential (log-Laplace) distribution [5]. Nevertheless, the proposed method can be applied to any jump-diffusion model described by some other distribution for both, finite and infinite activity. In the case of infinite activity, the integral term should be treated carefully by using, for instance, methods proposed in [23, 24].

We firstly immobilize the boundary using a front-fixing transformation because we are interested in the numerical solution not only of the price but also of the optimal exercise boundary separating the continuation region from the exercise zone.

Then the application of the method of lines, by using spatial semi-discretization of both the differential and integral parts transforms the PIDE problem into a system of nonlinear ordinary differential equations (ODEs) in time. For the spatial discretization of the differential part we use a centered FD scheme and for the discretization of the non-local integral part we use Gaussian quadrature rules instead of truncation plus trapezoidal rules or linear interpolation [23, 19].

Instead of a further direct full discretization, we use an exponential time differencing (ETD) method to approximate the solution of the integral equation equivalent to the system of ODEs [25, 26].

Tangman et al. in [27] use ETD scheme for solving European jump-diffusion models and the American option case is treated in [28] using the RBF method.

This paper is organized as follows. The problem is established in the following Section 2. Section 3 deals with the application of the front-fixing technique to transform the problem into a fixed-boundary PIDE problem where the optimal boundary becomes a new variable of the problem. Next Section 4 deals with the discretization of the problem in two steps. First, using spatial semi-discretization and then, an ETD technique to achieve the full discretization providing the approximations not only of the price, but also of the optimal exercise boundary. Due to the non-linearity and complexity of the problem, the analytical study of the qualitative properties of the proposed method becomes extremely difficult and tedious. Only few studies have performed Fourier stability analysis (see [20]) for the LCP formulation, which doses not include free boundary function to the PIDE. Thus, the empirical numerical stability and convergence are studied in Section 5. Conclusions are achieved throughout numerical experiments. The implementation of the proposed method has been done by using MatLab R2019b for Windows 10 home (64-bit) Intel(R) Core(TM) i5- 8265u CPU, 1.60 GHz.

2. Problem Statement: Jump-Diffusion Model

The most widely model used in the field of computational finance is the Black-Scholes model, which provides a simple computable pricing formula for European options in an ideal market. The model assumes that the underlying asset follows a geometric Brownian motion [29]. In its turn, American options offer to the holder the opportunity of early exercise, that makes the problem of American option pricing a challenging task and a question of great interest in the field.

Nevertheless, Black–Scholes model does not capture stock price fluctuations and market risks. These features can be taken into account by considering the following jump-diffusion model [4].

Let us consider the asset price S, that in the case of jumps satisfies the following stochastic differential equation (SDE)

$$\frac{dS}{S} = r dt + \sigma dW_t + (\eta - 1) dq, \tag{1}$$

where r is the risk free interest rate, σ is a volatility of the asset, dW_t is an increment of standard Wiener process W under the risk-neutral measure Q, dq is a Poisson process with intensity λ with

$$dq = \begin{cases} 0, \text{ with probability } 1 - \lambda dt, \\ 1, \text{ with probability } \lambda dt. \end{cases} \tag{2}$$

An impulse function producing jump from S to $S\eta$ is defined as $\eta - 1$ with the expected relative jump size $\kappa = \mathbb{E}(\eta - 1)$. Note that the jump rate $\lambda = 0$, SDE

(1) reduces to the geometric Brownian motion, that is a fundamental assumption of the Black-Scholes theory.

Then, the price $P(S,\tau)$ of the American put option under jump-diffusion model satisfies the following free-boundary partial integro-differential equation (PIDE) for $S > B(\tau)$, $0 < \tau \leq T$:

$$\frac{\partial P}{\partial \tau} = \frac{1}{2}\sigma^2 S^2 \frac{\partial^2 P}{\partial S^2} + (r - \lambda\kappa) S \frac{\partial P}{\partial S} - (r + \lambda) P + \lambda \int_0^\infty P(S\eta, \tau) g(\eta) d\eta, \quad (3)$$

where $\tau = T - t$ denotes the time to maturity T, and $g(\eta)$ is probability density function (PDF) of the jump with amplitude η, such that

$$g(\eta) \geq 0 \ \forall \eta, \quad \int_0^\infty g(\eta) d\eta = 1. \quad (4)$$

Initial condition (at $\tau = 0$) is defined by the type of option, and for a put is given by the following payoff function

$$P(S,0) = \max(E - S, 0), \ S \geq 0, \quad (5)$$

where E is the strike price.

Due to the early exercise privilege, the governing equation (3) is considered only in the holding region, i.e., for $S > B(\tau)$, where $B(\tau)$ is the early exercise boundary, not known a-priori. If the asset price $S \leq B(\tau)$ the optimal strategy is to exercise the option, i.e. the price of the option is defined by (5).

From the mathematical point of view, American option pricing problem is the free boundary PDE [30]. Thus, additional conditions are established:

$$B(0) = E, \qquad P(S,0) = \max(E - S, 0), \ S \geq 0, \quad (6)$$

$$\frac{\partial P}{\partial S}(B(\tau), \tau) = -1, \quad (7)$$

$$P(B(\tau), \tau) = E - B(\tau), \quad (8)$$

$$\lim_{S \to \infty} P(S, \tau) = 0, \quad (9)$$

In present paper, the two most widely used jump-diffusion models are considered: Merton's model based on lognormal distribution, and Kou's model represented by a log-double-exponential (log-Laplace) distribution. Nevertheless, the proposed method can be applied to any jump-diffusion model described by equations (3)–(4).

3. Front-Fixing Transformation

There are several useful techniques to treat the free boundary, including penalty method or formulation of linear complementarity problem. In present paper, we follow the front-fixing approach based on appropriate logarithmic transformation of PIDE resulting in new nonlinear equation with additional time-dependent unknown function. This approach demonstrates good results in accuracy and efficiency, moreover, it allows to describe the change of the domain in time, since the free boundary is explicitly found as a part of the solution.

In following we apply the front-fixing transformation to PIDE problem (3). Note that if $\lambda = 0$ and $\kappa = 0$, PIDE (3) reduces to Black-Scholes PDE. Thus, the American option pricing problem can be considered as a particular case of more general American jump-diffusion model.

Previous researches (see [31] and references therein) have suggested to apply the following dimensionless front-fixing transformation to treat the free boundary

$$x = \ln \frac{S}{B(\tau)}, \quad p(x,\tau) = \frac{P(S,\tau)}{E}, \quad S_{\mathrm{f}}(\tau) = \frac{B(\tau)}{E}. \tag{10}$$

In the case of jump-diffusion model (3), proposed front-fixing transformation (10) results in the following PIDE for $x > 0$, $0 < \tau \leq T$:

$$\frac{\partial p}{\partial \tau} = \frac{1}{2}\sigma^2 \frac{\partial^2 p}{\partial x^2} + \left(r - \lambda\kappa - \frac{\sigma^2}{2} \right) \frac{\partial p}{\partial x} + \frac{S_{\mathrm{f}}'}{S_{\mathrm{f}}} \frac{\partial p}{\partial x} - (r+\lambda)p + \lambda I(x,\tau), \tag{11}$$

where $I(x,\tau)$ is the following integral derived by introducing new variable $\xi = x + \ln \eta$,

$$I(x,\tau) = \int_{-\infty}^{+\infty} p(\xi) g(\exp(\xi - x)) \exp(\xi - x) d\xi. \tag{12}$$

Initial and boundary conditions take the form

$$S_{\mathrm{f}}(0) = 1, \qquad p(x,0) = 0,\ x \geq 0, \tag{13}$$

$$\frac{\partial p}{\partial x}(0,\tau) = -S_{\mathrm{f}}(\tau), \tag{14}$$

$$p(0,\tau) = 1 - S_{\mathrm{f}}(\tau), \tag{15}$$

$$\lim_{x\to\infty} p(x,\tau) = 0. \tag{16}$$

Such formulation of the jump-diffusion model of the option pricing has two important advantages: the PIDE problem can be solved numerically by employing any existing method, and the optimal stopping boundary can be calculated during the time looping of the numerical scheme. However, there are several computational difficulties related to the integral part approximation and the optimal stopping boundary calculation. Moreover, the solution of the problem should be found on the semi-infinite computational domain. In the following section we proposed numerical algorithm based on the ETD method paying special attention to the stated above challenges.

4. Exponential Time Differencing Method

In this section, we apply semi-discretization technique to transform the nonlinear PIDE to a system of ordinary differential equations, that is then solved by using ETD and matrix quadrature rules.

We consider the problem of American option pricing only in holding region. Thus, the problem (11)–(16) is defined on semi-infinite spatial interval $[0, +\infty)$. We truncate the domain by choosing $x_{\max}$ sufficiently large to guarantee the boundary condition (16). As it is shown in [32], in original variables, the choice of $S_{\max} = 3E$ is appropriate. However, option price could increase due to the jump-diffusion, leading to higher $S_{\max}$. Thus, in order to guarantee (16), we chose $x_{\max} = 3$. Hence, the numerical solution will be constructed in a computational domain $\Omega = [0, x_{\max}]$ with uniformly distributed spatial nodes x_j:

$$x_j = jh, \quad h = \frac{x_{\max}}{M}, \quad 0 \leq j \leq M. \tag{17}$$

Then, denoting an approximate solution at the point x_j by $p_j(\tau)$, the semi-discretization of the equation (11) is obtained by applying the second order central difference approximation for the spatial derivatives, resulting in the system of ODEs (for interior nodes, $1 \leq j \leq M-1$)

$$\begin{aligned} p_j' =& \frac{\sigma^2}{2} \frac{p_{j+1} - 2p_j + p_{j-1}}{h^2} + \left(r - \lambda\kappa - \frac{\sigma^2}{2} \right) \frac{p_{j+1} - p_{j-1}}{2h} \\ & - (r+\lambda) p_j + \frac{S_\mathrm{f}'}{S_\mathrm{f}} \frac{p_{j+1} - p_{j-1}}{2h} + \lambda I(x_j, \tau). \end{aligned} \tag{18}$$

Approximation of the integral term is denoted by $I_j \approx I(x_j, \tau)$ and computed by the Gauss–Hermite quadrature in the following form

$$I_j = \sum_{i=0}^{N_q} \omega_i e^{\xi_i^2} \hat{p}(\xi_i, \tau) g(e^{\xi_i - x_j}) e^{\xi_i - x_j}, \tag{19}$$

where N_q is the number of sample points, ξ_i are the roots of the physicists' version of the Hermite polynomial $H_{N_q}(\xi)$ with the associated weights ω_i, $i = 1, 2, \ldots, N_q$. Values $\hat{p}(\xi_i, \tau)$ can be found by using interpolation of the numerical solution at the moment τ or from the boundary conditions, depending on ξ_i, $i = 1, 2, \ldots, N_q$:

1. $\xi_i \leq 0$, then the transformed payoff function is used: $\hat{p}(\xi_i, \tau) = 1 - e^{\xi_i} S_\mathrm{f}(\tau)$;
2. $0 < \xi_i < x_{\max}$, then the interpolation of the numerical solution is used;
3. $\xi_i \geq x_{\max}$, then, according to boundary conditions, the value is zero.

As a result, the integral term I_j can be written as a linear combination of functions $p(x, \tau)$, including some free components.

Central finite difference of the second order is applied to the boundary condition (14) resulting in the following FD equation

$$\frac{p_1(\tau) - p_{-1}(\tau)}{2h} = -S_\mathrm{f}(\tau), \tag{20}$$

where $p_{-1}(\tau) = p(-h, \tau)$ is the value at an auxiliary point out of the domain.

We assume that equation (11) holds at $x = 0$ and due to boundary conditions (14)–(15) takes the following form

$$\frac{\sigma^2}{2}\frac{\partial^2 p}{\partial x^2}(0,\tau) + \left(\frac{\sigma^2}{2} + \lambda(\kappa+1)\right) S_{\mathrm{f}}(\tau) - (r+\lambda) + \lambda I(0,\tau) = 0. \tag{21}$$

We estimate the value at this point assuming that (21) holds for American vanilla option[33, 34], i.e., FD equation (18) is fulfilled for $j = 0$, taking $\lambda = 0$. Then, the following relation could be established

$$p_1(\tau) = \alpha - \beta S_{\mathrm{f}}(\tau), \tag{22}$$

where

$$\alpha = 1 + \frac{rh^2}{\sigma^2}, \quad \beta = 1 + h + \frac{h^2}{2}. \tag{23}$$

Differentiating (22) with respect to τ, we obtain ODE:

$$p_1'(\tau) = -\beta S_{\mathrm{f}}'(\tau). \tag{24}$$

From (22) and (15) one gets

$$p_0(\tau) = \frac{1}{\beta}\left(\beta - \alpha + p_1(\tau)\right), \quad \tau > 0. \tag{25}$$

The nonlinear system (18) contains $M-1$ ODEs for M unknown functions ($p_j(\tau)$, $j = 1, \ldots, M-1$, and $S_{\mathrm{f}}(\tau)$). To close up the system, equations (22) and (24) can be considered in the following form

$$\frac{S_{\mathrm{f}}'}{S_{\mathrm{f}}} = -\frac{p_1'}{\alpha - p_1}, \tag{26}$$

that allows to exclude $S_{\mathrm{f}}(\tau)$ from the system.

Hence, taking into account (25) and (26), system(18) finally takes the form

$$\begin{cases} p_1' = \left[\frac{\sigma^2}{2h^2}\left(p_0 - 2p_1 + p_2\right) + \gamma\frac{p_2 - p_0}{2h} - (r+\lambda)p_1 + \lambda I_1\right]\frac{\alpha - p_1}{\alpha - p_1 + \frac{p_2 - p_0}{2h}}, \\ p_2' = \frac{\sigma^2}{2h^2}\left(p_1 - 2p_2 + p_3\right) + \gamma\frac{p_3 - p_1}{2h} - (r+\lambda)p_2 - \frac{p_1'}{\alpha - p_1}\frac{p_3 - p_1}{2h} + \lambda I_2, \\ \ldots \\ p_j' = \frac{\sigma^2}{2h^2}\left(p_{j-1} - 2p_j + p_{j+1}\right) + \gamma\frac{p_{j+1} - p_{j-1}}{2h} - (r+\lambda)p_j - \frac{p_1'}{\alpha - p_1}\frac{p_{j+1} - p_{j-1}}{2h}\lambda I_j, \\ \ldots \\ p_{M-1}' = \frac{\sigma^2}{2h^2}\left(p_{M-2} - 2p_{M-1}\right) - \gamma\frac{-p_{M-2}}{2h} - (r+\lambda)p_{M-1} + \frac{p_1'}{\alpha - p_1}\frac{p_{M-2}}{2h} + \lambda I_{M-1}, \end{cases} \tag{27}$$

where $\gamma = r - \lambda\kappa - \frac{\sigma^2}{2}$, and

$$p_0 = \begin{cases} 0, & \tau = 0, \\ \frac{\beta - \alpha + p_1}{\beta}, & \tau > 0. \end{cases} \tag{28}$$

System (27) is written in the matrix form

$$\bar{p}' = A\bar{p} + \Phi(\bar{p}), \tag{29}$$

where $\bar{p} = [p_1, \ldots, p_{M-1}]^T$, where $\Phi(\bar{p})$ is the vector that contains nonlinear part of the equations, A is the $(M-1) \times (M-1)$ matrix of coefficients. The interpolation used in Gauss-Hermite quadrature lead to a linear combination of terms p_j and some free components. The coefficients of this linear combination contribute to the matrix A, while the free component is included into the nonlinear part. Thus, matrix A can written as a sum of one tridiagonal matrix (of the central FD scheme) A_{FD} :

$$A_{\text{FD}} = \begin{pmatrix} 0 & 0 & 0 & \ldots & 0 & 0 & 0 \\ a_{-1} & a_0 & a_{+1} & \ldots & 0 & 0 & 0 \\ \ddots & \ddots & \ddots & \ddots & \ddots & \ddots & \ddots \\ 0 & 0 & 0 & \ddots & 0 & a_{-1} & a_0 \end{pmatrix} \tag{30}$$

of coefficients

$$a_{\pm 1} = \frac{\sigma^2}{2h^2} \pm \left(r - \lambda\kappa - \frac{\sigma^2}{2} \right) \frac{1}{2h}, \quad a_0 = -\frac{\sigma^2}{h^2} - (r + \lambda), \tag{31}$$

and one matrix of interpolation coefficients A_{Int}, such that $A = A_{\text{FD}} + A_{\text{Int}}$.

The nonlinear part is written

$$\Phi(\bar{p}) = \begin{pmatrix} \phi(\alpha - p_1) \\ -\phi\frac{p_3 - p_1}{2h} + \lambda \hat{I}_2 \\ \cdots \\ -\phi\frac{p_{j+1} - p_{j-1}}{2h} + \lambda \hat{I}_j \\ \cdots \\ \phi\frac{p_{M-2}}{2h} + \lambda \hat{I}_{M-1} \end{pmatrix}, \tag{32}$$

denoting

$$\phi = \left[\frac{\sigma^2}{2h^2}(p_0 - 2p_1 + p_2) + \gamma\frac{p_2 - p_0}{2h} - (r+\lambda)p_1 + \lambda\hat{I}_1\right]\frac{1}{\alpha - p_1 + \frac{p_2-p_0}{2h}}, \tag{33}$$

where $\hat{I}$ stands for the free terms of the Gauss-Hermite quadrature.

Nonlinear system of ODEs (29) represents the behaviour in time of the transformed price function and can be solved numerically by ETD method [26]. The idea of the method is to use matrix exponential and exact integration of linear part of the equation. For the temporal discretization we fix the time step $k = \frac{T}{N}$, so that $\tau^n = nk$, $n = 0, \ldots, N$.

Since A in (29) does not depend on $\bar{p}$ and $\Phi(\bar{p})$ is a nonlinear term, we multiply both parts of (29) by the integrating factor $e^{-A\tau}$ and integrate over time τ from τ^n to τ^{n+1}:

$$e^{-A\tau^{n+1}}\bar{p}(\tau^{n+1}) - e^{-A\tau^n}\bar{p}(\tau^n) = \int_{\tau^n}^{\tau^{n+1}} e^{-A\tau}\Phi(\bar{p}(\tau))d\tau. \tag{34}$$

Taking into account $k = \tau^{n+1} - \tau^n$ and changing the variable in the integral $s = \tau^{n+1} - \tau$ one gets

$$\bar{p}(\tau^{n+1}) = e^{Ak}\bar{p}(\tau^n) + \int_0^k e^{As}\Phi(\bar{p}(\tau^{n+1} - s))ds. \tag{35}$$

Note that the integral equation (35) is equivalent to the system of ODE (29) in some given interval $s \in [\tau^n, \tau^{n+1}]$, see for details Section 2.1 of [26].

We propose a first explicit approximation of the integral in (35) by replacing $\bar{p}(\tau^{n+1} - s)$ by the known value $\bar{p}(\tau^n)$ that corresponds to $s = k$. The local truncation error of such approximation is $O(k^2)$ [26]. Then (35) takes the form

$$\bar{p}(\tau^{n+1}) = e^{Ak}\bar{p}(\tau^n) + \left(\int_0^k e^{As}ds\right)\Phi(\bar{p}(\tau^n)). \tag{36}$$

Matrix A is singular and does not have a matrix inverse. Thus, in order to avoid the computation of A^{-1} in exact computation of the integral $\int_0^k e^{As}ds$ [35], Simpson's quadrature rule is used [36]:

$$\int_0^k e^{As}ds = \frac{k}{6}\left(e^{Ak} + 4e^{A\frac{k}{2}} + I\right) + O(k^5), \tag{37}$$

where I stands for the identical matrix of size $M-1$.

5. Numerical Analysis and Examples

This section deals with empirical numerical analysis of the proposed method for various models including study of numerical stability as one of the most important characteristics of a numerical scheme.

Based on previous studies [31, 37], we aim to estimate the stability condition on step sizes. It is found that in the case of European option, i.e. without free boundary, the FD Euler scheme contains positive coefficients, if

$$h < \frac{\sigma^2}{|r - \lambda\kappa - \sigma^2/2|}, \quad k < \frac{h^2}{\sigma^2 + (r+\lambda)h^2}. \tag{38}$$

In present paper, we consider (38) as reference conditions for the numerical study of stability of the proposed method. The second condition of (38) can be written as

$$k < C_{\mathrm{ref}}(h) \cdot h^2, \qquad C_{\mathrm{ref}}(h) = \frac{1}{\sigma^2 + (r+\lambda)h^2}. \tag{39}$$

Further, we provide series of experiments varying time step $k = C \cdot h^2$ in order to establish numerically the critical value C_{critical} and compare it with the theoretical C_{ref}.

5.1. American Vanilla Option

First, let us check the stability condition (38) for the American option case, i.e., for $\lambda = 0$ and $\kappa = 0$. If $C = C_{\mathrm{critical}} + \varepsilon$, $(\varepsilon > 0)$ is chosen, small perturbations are observed in the solution. However, starting from $h = 0.003$ the stability criterion becomes much stricter, and even small ε in $C = C_{\mathrm{critical}} + \varepsilon$ leads to huge oscillations and very unstable solution (compare Figures 1 and 2).

We estimate the impact of the parameters r and σ on stability of the proposed method (in terms of C_{critical}) by repeating the experiment described above with one fixed parameter and varying an other. Critical values of C are found numerically and presented in Table 1 and plotted in Figure 3 together with the theoretical values C_{ref}. Note that C_{ref} are found to have slight dependence on r, while computed values, especially for small h, varies. However, for h sufficiently

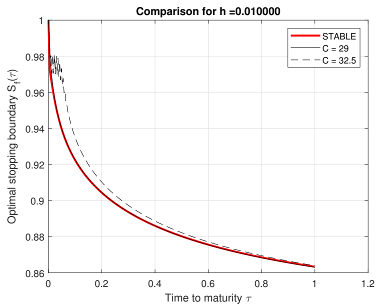

Figure 1: Optimal stopping boundary for the problem with parameters (40) by the proposed method (ETD) with $h = 0.01$, and $k = Ch^2$, where $C = 29$ (that is found to be critical) and $C = 32.5$.

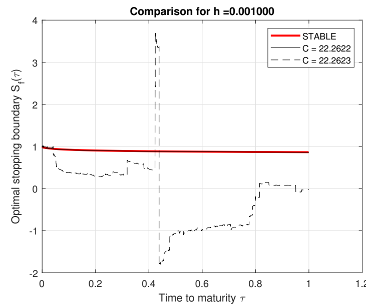

Figure 2: Optimal stopping boundary for the problem with parameters (40) by the proposed method (ETD) with $h = 0.001$, and $k = Ch^2$, where $C = 22.262$ ($C_{\text{critical}} = 22.262$) and $C = 22.2623$.

large, the range of computed critical values of C is fixed and the theoretical C are less than the computed. Thus, in the case of American Vanilla option, (38) can be considered as a stability condition.

Now, let us fix $r = 0.1$ and check the impact of the volatility on the stability. Critical values C_{critical} are collected in Table 2 and presented in Figure 4. Observing the plots, we found that C_{critical} depends on σ, but almost does not change across h-axe. The theoretical values C_{ref} plotted in red are found to be less than computed values for h sufficiently large. With increasing σ both lines are approximating to each other.

Example 5.1. *The American option without jumps considered in [33] takes the following parameters*

$$r = 0.1; \quad \sigma = 0.2; \quad E = 100; \quad T = 1. \tag{40}$$

For the transformed problem (10)–(16) with parameters(40) we set $x_{\max} = \ln 3$, that corresponds to the choice $S_{\max} = 3E$ at the initial moment. The numerical solution is constructed with $h = 10^{-2}$ and $k = 10^{-4}$. The proposed method is compared with the finite-difference method of [31] and with results

$h \backslash r$	0.01	0.025	0.05	0.1
0.003	15.0	18.0	22.0	22.0
0.005	17.0	22.0	22.0	24.0
0.007	18.0	22.0	23.0	30.0
0.009	18.0	22.0	23.0	30.0
0.01	18.0	22.0	24.0	30.0
0.02	22.0	24.0	30.0	31.0
0.03	22.0	30.0	31.0	31.0
0.04	23.0	30.0	31.0	30.0
0.05	24.0	30.0	31.0	30.0
0.06	30.0	31.0	30.0	30.0
0.07	30.0	31.0	30.0	29.0
0.08	30.0	31.0	30.0	29.0
0.09	31.0	30.0	30.0	28.0
0.1	31.0	30.0	30.0	28.0

Table 1: Empirical critical values of C depending on h for various r with fixed $\sigma = 0.2$.

$h \backslash \sigma$	0.1	0.2	0.3	0.4	0.5
0.003	123.0	22.0	9.0	4.0	2.0
0.005	126.0	24.0	10.0	5.0	2.0
0.007	125.0	30.0	10.0	5.0	3.0
0.009	124.0	30.0	10.0	5.0	3.0
0.01	124.0	30.0	10.0	5.0	3.0
0.02	119.0	31.0	13.0	6.0	3.0
0.03	115.0	31.0	13.0	7.0	3.0
0.04	111.0	30.0	13.0	7.0	4.0
0.05	108.0	30.0	13.0	7.0	4.0
0.06	104.0	30.0	13.0	7.0	4.0
0.07	101.0	29.0	13.0	7.0	4.0
0.08	299.0	29.0	13.0	7.0	4.0
0.09	299.0	28.0	13.0	7.0	4.0
0.1	299.0	28.0	13.0	7.0	4.0

Table 2: Empirical critical values of C depending on h for various $\sigma = 0.1$ and fixed $r = 0.1$.

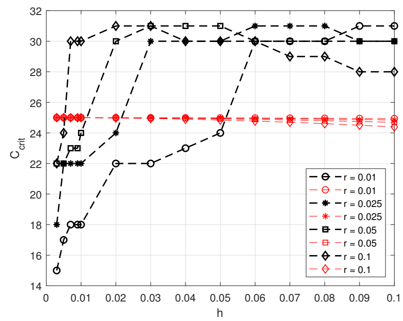

Figure 3: Stability condition $k \leq Ch^2$ depending on h for various r and fixed $\sigma = 0.2$. Black lines are for the computed critical values, while C_{ref} (39) are presented in red.

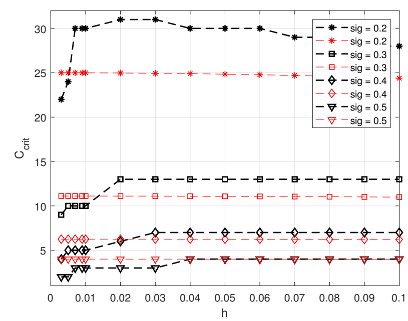

Figure 4: Stability condition $k \leq Ch^2$ depending on h for various σ and fixed $r = 0.1$. Black lines are for the computed critical values, while C_{ref} (39) are presented in red.

Method	$S_{\text{f}}(T)$
FF-ETD (proposed)	0.8628
FF-FDM [31]	0.8628
FF-Expl [33]	0.8623
FF-Impl [33]	0.8619

Table 3: Optimal stopping boundary at the moment of signing the contract $\tau = T$ computed by the proposed FF-ETD method and FD method proposed in [31, 33].

of [33] in Table 3.

The numerical solution of the problem is constructed as described above by using the ETD method. Then the inverse transform is applied to the solution in order to obtain the option price at the moment $\tau = T$, i.e. at the moment of signing the contract. The numerical solution (solid line) and the payoff (dashed lined) are presented in Figure 5. It can be noticed that the numerical solution is constructed not in the whole interval $[0, S_{\max}]$, but from the optimal stopping boundary. The change of $S_{\text{f}}(\tau)$ in time is given in Figure 6 comparing with the results of the proposed in [31] FDM with logarithmic front-fixing transformation.

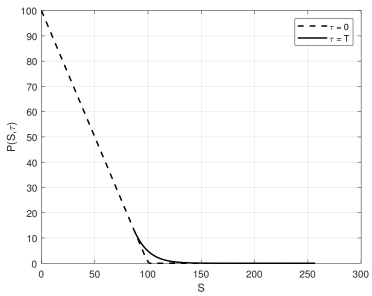

Figure 5: Prices of American option with parameters (40) at initial moment ($\tau = 0$) and numerical solution by the proposed ETD method with $h = 0.01$, $k = h^2$ at moment $\tau = T$.

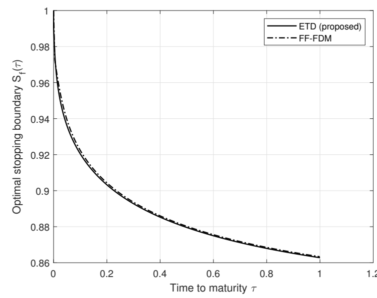

Figure 6: Optimal stopping boundary by the proposed method (ETD) with $h = 0.01$, $k = h^2$ and the FDM from [31] for the problem with parameters (40).

5.2. Merton's Model

Under Merton's model $g(\eta)$ is the PDF of the lognormal distribution with parameters μ_J and σ_J:

$$g_{\text{Merton}}(\eta) = \frac{1}{\sqrt{2\pi}\sigma_J \eta} \exp\left(-\frac{(\ln \eta - \mu_J)^2}{2\sigma_J^2}\right). \tag{41}$$

In the case of lognormal distribution with the mean μ_J and the variance σ_J^2, the expected relative jump size takes the form

$$\kappa_{\text{Merton}} = \mathbb{E}(\eta - 1) = \exp\left(\mu_J + \frac{\sigma_J^2}{2}\right) - 1. \tag{42}$$

In the case of Merton's model, under the front-fixing transformation the integral term (12) takes the form

$$I_{\text{Merton}}(x,\tau) = \frac{1}{\sqrt{2\pi}\sigma_J} \int_{-\infty}^{+\infty} p(\xi,\tau) \exp\left(-\frac{(\xi - (x+\mu_J))^2}{2\sigma_J^2}\right) d\xi, \tag{43}$$

that can be understood as an expectation of $p(x,\tau)$ for normally distributed x with mean $x + \mu_J$ and the standard deviation σ_J.

The integral term given in form (43) requires an additional change of variable. For every fixed j let us consider $\gamma_i = \frac{\xi_i - x_j - \mu_J}{\sqrt{2\pi}\sigma_J}$, then

$$(I_{\text{Merton}})_j^n = \frac{1}{\sqrt{\pi}} \sum_{i=0}^{N_q} \omega_i \hat{p}(\sqrt{2}\sigma_J \gamma_i + (\mu_J + x_j), \tau^n). \tag{44}$$

In present section we consider several numerical examples in order to study the numerical stability of the solution, as well as to compare the proposed FDM based on the front-fixing transformation with known methods in literature.

Example 5.2. *American put option under the Merton model with parameters [38]*

$$\begin{aligned} \sigma = 0.15,\ r = 0.05,\ T = 0.25,\ E = 100, \\ \lambda = 0.1,\ \sigma_J = 0.45,\ \mu_J = -0.9. \end{aligned} \tag{45}$$

This set of parameters is used for comparison by many authors [28]. In Table 4 the price of American option (45) at $S = E$ is given. For numerical solution we chose $x_{\max} = 3$, $N_q = 10$. We compare the proposed method (FF-ETD) with the cubic spline radial basis function method (RBF-CH) of Chan and Hubbert [39]; proposed in [28] radial basis function with differential quadrature with exponential time integration (RBF-ETI). In the case of the FF-ETD method, more spatial nodes are necessary to reach the desired accuracy. Thus, for $N = 1600$, the option price is $P(E, 0) = 3.2413$. In [11], the operator splitting FDM method (OS-FDM) is proposed, with the most accurate estimation of the option price with parameters (45), equal to 3.2441229 obtained with $N = 4096$ spatial nodes. As a reference value the results of the implicit method by d'Halluin et al. [40] is chosen. As one can see from the results, in some cases RBF methods may perform better than the proposed method. However, their efficiency and robustness is very sensitive to the choice of shape parameter and the RBF method does not provide a strategy to select the appropriate values of it.

To compare the convergence of the proposed method, the relative error is considered. From the results presented in Figure 7 we can conclude that the FF-ETD method shows almost quadratic convergence in space. To be more precisely, we compute the convergence rate $\gamma(n_1, n_2)$ by the following formula

N	FF-ETD (proposed)	RBF-CH [39]	RBF-ETI [28]
80	3.3133	3.9833	3.2873
160	3.2618	3.3803	3.2515
320	3.2463	3.2084	3.2437
640	3.2428	3.1658	3.2418
Reference value	3.241248		

Table 4: Comparison of prices of American put option with parameters (45) at $S = 100$ using the proposed method and RBF methods of [28] and [39] for various number of spatial grid nodes N (temporal step size k is fixed).

$$\gamma(N_1, N_2) = \frac{\log(error_1) - \log(error_2)}{\log(N_2) - \log(N_1)}, \tag{46}$$

where *error* stands for the relative error for the results in Table 4. For instance, for $N_1 = 320$ and $N_2 = 640$, $\gamma(320, 640) = 2.1394$, while $\gamma(80, 160) = 1.8061$ that gives the average value $\bar{\gamma} = 1.9906$.

In order to check condition (39), the following cases are simulated:

1. $C \ll C_{\text{ref}}$ ($C = 0.01C_{\text{ref}}$);
2. $C < C_{\text{ref}}$ ($C = 0.9C_{\text{ref}}$);
3. $C = C_{\text{ref}}$;
4. $C > C_{\text{ref}}$ ($C = 1.28C_{\text{ref}}$).

The free boundary motion for these C are given in Figure 8. The number of spatial nodes is 600, in that case for parameters (45), $C_{\text{ref}}(h) = 44.4370$. Even the perturbations in C are not significant, but if the condition (38) is broken (case 3), the solution is not stable, that confirms condition 39.

5.3. Kou's Model

Under Kou's model $g(\eta)$ is the PDF of the log-Laplace density:

$$g_{\text{Kou}}(\eta) = \begin{cases} q\alpha_2\eta^{\alpha_2 - 1}, & 0 < \eta < 1, \\ (1-q)\alpha_1\eta^{-(\alpha_1+1)}, & \eta \geq 1, \end{cases} \tag{47}$$

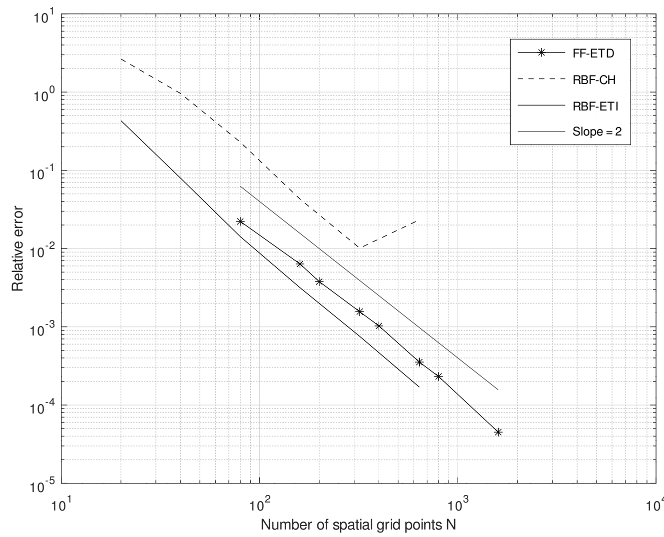

Figure 7: The relative error depending on number of spatial nodes for various methods from Table 4.

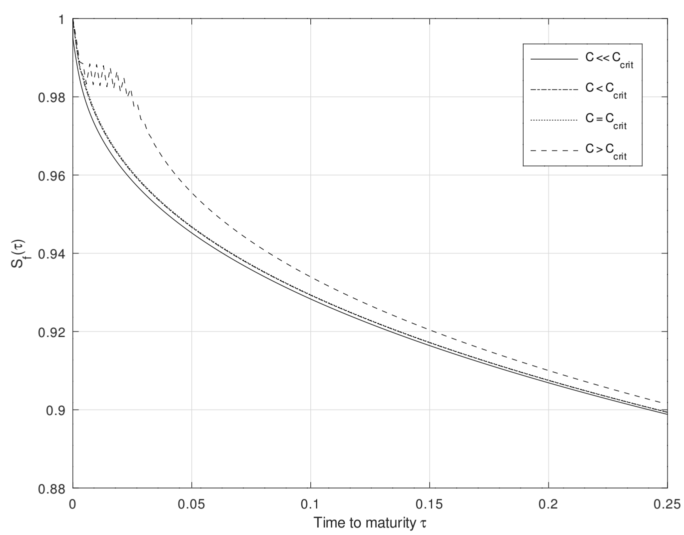

Figure 8: Optimal stopping boundary S_{f} under the Merton's model computed by the FF-ETD method with various C.

N	FF-ETD	CPU-time (s)
100	2.841335	0.2656
200	2.812952	0.9062
400	2.810183	1.1406
800	2.808384	5.8280
1600	2.807821	105.4884
Reference value	2.807879	

Table 5: Comparison of prices of American put option with parameters (49) at $S = 100$ using the FF-ETD for various number of spatial grid nodes N with corresponding CPU-time.

where $\alpha_1 > 1$, $\alpha_2 > 0$ and $0 < q < 1$ are parameters of the log double exponential distribution. In that case, the expected relative jump size can be found as follows

$$\kappa_{\mathrm{Kou}} = \frac{(1-q)\alpha_1}{\alpha_1 - 1} + \frac{q\alpha_2}{\alpha_2 + 1} - 1. \tag{48}$$

Example 5.3. *The proposed method is applied to price American put option under Kou's model, the parameters are given in [19, 9]:*

$$\begin{gathered} \sigma = 0.15,\ r = 0.05,\ T = 0.25,\ E = 100, \\ \lambda = 0.1,\ \alpha_1 = 3.0465,\ \alpha_2 = 3.0775,\ q = 0.6555. \end{gathered} \tag{49}$$

Table 5 reports the results for the proposed FF-ETD method reporting the corresponding CPU-time. To obtain these results, the following parameters of discretization are used: $x_{\max} = 3$, $N_q = 8$. In order to guarantee the stability of the method, temporal step size has to be chosen as $k < C_{\mathrm{ref}} h^2$, we set $C = 1 < C_{\mathrm{ref}}$.

In order to establish the convergence rate of the FF-ETD method we set $k = 3.5 \cdot 10^{-6}$ and repeat the simulations described above for $N = 100, \ldots, 1600$. Using formula (46), the mean value $\bar{\gamma} = 2.0373$.

The convergence of the proposed method is compared analogously to the previous example. The results are given in Figure 9. The FF-ETD is compared

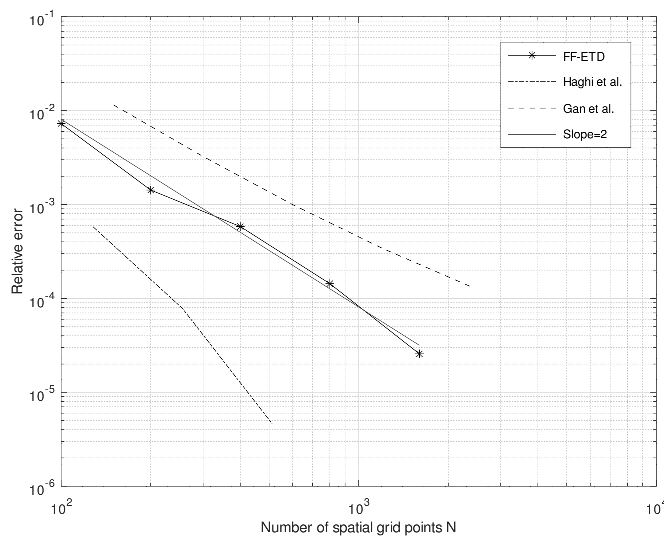

Figure 9: The relative error depending on number of spatial nodes for the FF-ETD method (with fixed time-step $k = 3.5 \cdot 10^{-6}$), finite volume method proposed by Gan et al. in [9], and RBF-FD method proposed by Haghi et al. in [22].

with the penalty method treated by finite volume method proposed in [9], and of the RBF-FD method of [22]. As a reference value the solution of [19] on the refined grid is used. In the case of Kou's model, the FF-ETD method shows the second order of convergence.

Analogously to the previous example, we check stability condition (39) by running the algorithm with various C. The free boundary motion for these C are given in Figure 10. The number of spatial nodes is 600, in that case for parameters (49), $C_{\text{ref}}(h) = 44.4370$. Again, if the condition (39) is broken ($C = 1.1C_{\text{ref}}$), the solution is not stable, as it has been expected. However, it is found that the FF-ETD method for the Kou's model is more sensitive to the stability condition (39), because in that case even small increment in C_{ref} leads to the instability.

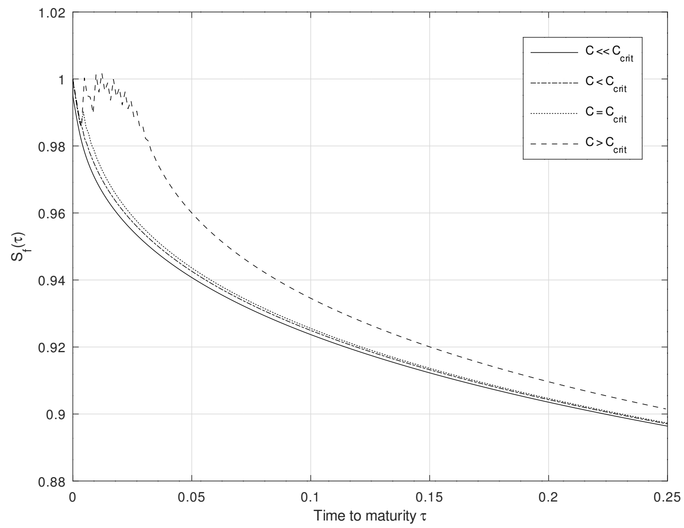

Figure 10: Optimal stopping boundary S_{f} under the Kou's model computed by the FF-ETD method with various C.

6. Conclusion

Numerical solution for the American option pricing problem under jump-diffusion is challenging task due to the free boundary and additional integral term. In this paper, the free boundary is treated by the front-fixing method, while the integral part is accurately approximated by the Hermite-Gauss quadrature. The PIDE has been then solved by ETD method.

The FF-ETD method can be applied to a PIDE. The front-fixing approach allows to incorporate the free boundary as an additional unknown function. The method shows the second order of convergence in space. Since matrix A is constant-valued, the computation of the matrix exponential is needed just once for all time steps. Moreover, the stability conditions for the proposed FF-ETD are weaker than ones for the standard explicit FDM, which leads to the smaller number of time iterations. Thus, the proposed method requires less computational resources comparing to FD method.

Proposed method is applied to two widely used jump-diffusion models, Merton's model and Kou's model. The method is analysed numerically. Established stability condition is shown empirically for both cases, as well as for the American vanilla option, without integral term. The convergence rate is computed and compared with relevant methods in the literature that shows its competitiveness.

Aknowledgements

This work has been partially supported by the Ministerio de Ciencia, Innovación y Universidades, Spanish grant MTM2017-89664-P.

References

[1] P. Carr, L. Wu, What Type of Process Underlies Options? A Simple Robust Test, The Journal of Finance 58 (6) 2581–2610 (2003). doi:10.1046/j.1540-6261.2003.00616.x.

[2] J. Pan, The jump-risk premia implicit in options: evidence from an integrated time-series study, Journal of Financial Economics 63 (1) 3–50 (2002). doi:10.1016/S0304-405X(01)00088-5.

[3] P. Cont, R. and Tankov, Financial Modelling With Jump Processes, Chapman & Hall/CRC Financial Mathematics Series (Boca Raton, Fla., London: Chapman & Hall/CRC) (2004).

[4] R. C. Merton, Option pricing when underlying stock returns are discontinuous, Journal of Financial Economics 3 (1-2) 125–144 (1976). doi:10.1016/0304-405X(76)90022-2.

[5] S. G. Kou, A Jump-Diffusion Model for Option Pricing, Management Science 48 (8) 1086–1101 (2002). doi:10.1287/mnsc.48.8.1086.166.

[6] Y. K. Kwok, Mathematical Models of Financial Derivatives, Springer (2008).

[7] Y. Huang, P. Forsyth, G. Labahn, Inexact arithmetic considerations for direct control and penalty methods: American options under jump diffusion, Applied Numerical Mathematics 72 33–51 (2013). doi:10.1016/J.APNUM.2013.02.007.

[8] Y. D'Halluin, P. A. Forsyth, G. Labahn, A penalty method for American options with jump diffusion processes, Numerische Mathematik 97 (2) 321–352 (2004). doi:10.1007/s00211-003-0511-8.

[9] X. Gan, Y. Yang, K. Zhang, A robust numerical method for pricing American options under Kou's jump-diffusion models based on penalty method, Journal of Applied Mathematics and Computing 62 (1) 1–21 (2020). doi:10.1007/s12190-019-01270-1.

[10] S. Ikonen, J. Toivanen, Operator splitting methods for American option pricing, Applied Mathematics Letters 17 (7) 809–814 (2004). doi:10.1016/j.aml.2004.06.010.

[11] Y. Kwon, Y. Lee, A second-order tridiagonal method for American options underjump-diffusion models, SIAM Journal on Scientific Computing 33 (4) 1860–1872 (2011). doi:10.1137/100806552.

[12] A. Golbabai, D. Ahmadian, M. Milev, Radial basis functions with application to finance: American put option under jump diffusion, Mathematical and Computer Modelling 55 (3-4) 1354–1362 (2012). doi:10.1016/J.MCM.2011.10.014.

[13] S. Heidari, H. Azari, A front-fixing finite element method for pricing American options under regime-switching jump-diffusion models, Computational and Applied Mathematics 37 (3) 3691–3707 (2018). doi:10.1007/s40314-017-0540-z.

[14] M. Broadie, Ö. Kaya, Exact simulation of stochastic volatility and other affine jump diffusion processes, Operations Research 54 (2) 217–231 (2006). doi:10.1287/opre.1050.0247.

[15] F. D'Ippoliti, E. Moretto, S. Pasquali, B. Trivellato, Exact and approximated option pricing in a stochastic volatility jump-diffusion model, in: M. Corazza, C. Pizzi (Eds.), Mathematical and Statistical Methods for Actuarial Sciences and Finance, Springer Milan, Milano, 133–142 (2010).

[16] L. V. Ballestra, C. Sgarra, The evaluation of American options in a stochastic volatility model with jumps: an efficient finite element approach, Computers & Mathematics with Applications 60 (6) 1571–1590 (2010). doi:10.1016/j.camwa.2010.06.040.

[17] L. V. Ballestra, L. Cecere, A fast numerical method to price American options under the Bates model, Computers & Mathematics with Applications 72 (5) 1305–1319 (2016). doi:10.1016/j.camwa.2016.06.041.

[18] C. Chiarella, B. Kang, G. H. Mayer, A. Ziogas, C. Ciarella, B. Kang, G. H. Meyer, A. Ziogas, The evaluation of American option prices under stochastic volatility and jump-diffusion dynamics using the method of lines, International Journal of Theoretical and Applied Finance 12 (03) 393–425 (2009). doi:10.1142/S0219024909005270.

[19] S. Salmi, J. Toivanen, An iterative method for pricing American options under jump-diffusion models, Applied Numerical Mathematics 61 (7) 821–831 (2011). doi:10.1016/J.APNUM.2011.02.002.

[20] S. Salmi, J. Toivanen, IMEX schemes for pricing options under jump–diffusion models, Applied Numerical Mathematics 84 33–45 (2014). doi:10.1016/J.APNUM.2014.05.007.

[21] M. K. Kadalbajoo, A. Kumar and L. P. Tripathi, A radial basis function based implicit–explicit method for option pricing under jump-diffusion models, Applied Numerical Mathematics 110 159 - 173 (2016). doi: 10.1016/J.APNUM.2016.08.006.

[22] M. Haghi, R. Mollapourasl, M. Vanmaele, An RBF–FD method for pricing American options under jump–diffusion models, Computers & Mathematics

with Applications 76 (10) 2434–2459 (2018). doi:10.1016/J.CAMWA.2018.08.040.

[23] R. Cont, E. Voltchkova, A finite difference scheme for option pricing in jump diffusion and exponential Lévy models, SIAM Journal on Numerical Analysis 43 (4) 1596–1626 (2006). doi:10.1137/S0036142903436186.

[24] M. Fakharany, R. Company, L. Jódar, Solving partial integro-differential option pricing problems for a wide class of infinite activity Lévy processes, Journal of Computational and Applied Mathematics 296 739–752 (2016). doi:10.1016/J.CAM.2015.10.027.

[25] A. Pazy, Semigroups of Linear Operators and Applications to Partial Differential Equations, Springer (1983).

[26] S. Cox, P. Matthews, Exponential time differencing for stiff systems, Journal of Computational Physics 176 (2) 430–455 (2002). doi:10.1006/JCPH.2002.6995.

[27] D. Y. Tangman, A. Gopaul, M. Bhuruth, A fast high-order finite difference algorithm for pricing American options, Journal of Computational and Applied Mathematics 222 (1) 17–29 (2008). doi:10.1016/j.cam.2007.10.044.

[28] A. A. E. F. Saib, D. Y. Tangman, M. Bhuruth, A new radial basis functions method for pricing American options under Merton's jump-diffusion model, International Journal of Computer Mathematics 89 (9) 1164–1185 (2012). doi:10.1080/00207160.2012.690034.

[29] J. Hull, Options, Futures and Other Derivatives, Pearson/Prentice Hall (2009).

[30] P. Wilmott, S. Howison, J. Dewynne, The Mathematics of Financial Derivatives, Cambridge University Press, Cambridge, UK (1995).

[31] R. Company, V. Egorova, L. Jódar, Solving American option pricing models by the front fixing method: Numerical analysis and computing, Abstract and Applied Analysis (2014). doi:10.1155/2014/146745.

[32] R. Kangro, R. Nicolaides, Far field boundary conditions for Black–Scholes equations, SIAM Journal on Numerical Analysis 38 (4) 1357–1368 (2000). doi:10.1137/S0036142999355921.

[33] Nielsen B.F., Skavhaug O., A. Tvelto, Penalty and front-fixing methods for the numerical solution of American option problems, Journal Of Computational Finance 5(4) 69–97 (2002). doi:10.21314/JCF.2002.084.

[34] L. Wu, Y.-K. Kwok, A front-fixing method for the valuation of American option, The Journal of Financial Engineering 6 83–97 (1997).

[35] N. Rambeerich, D. Tangman, M. Lollchund, M. Bhuruth, High-order computational methods for option valuation under multifactor models, European Journal of Operational Research 224 (1) 219–226 (2013). doi:10.1016/J.EJOR.2012.07.023.

[36] K. Atkinson, An Introduction to Numerical Analysis, 2nd Edition, John Wiley & Sons (1989).

[37] R. Company, V. N. Egorova, L. Jódar, Conditional full stability of positivity-preserving finite difference scheme for diffusion–advection-reaction models, Journal of Computational and Applied Mathematics 341 157–168 (2018). doi:10.1016/J.CAM.2018.02.031.

[38] J. Andersen, Leif B.G. and Andreasen, Jump-Diffusion Processes: Volatility Smile Fitting and Numerical Methods for Pricing, Review of Derivatives Research, 4 (3) 231–262 (2000) doi:10.1023/A:1011354913068.

[39] R. T. L. Chan, S. Hubbert, A Numerical study of radial basis function based methods fo options pricing under the one dimension jump-diffusion model ArXiv abs/1011.5650 (2010) arXiv:1011.5650.

[40] Y. D'Halluin, P. A. Forsyth, K. R. Vetzal, Robust numerical methods for contingent claims under jump diffusion processes, IMA Journal of Numerical Analysis 25 (1) 87–112 (2005). doi:10.1093/imanum/drh011.